Naval Research Laboratory

Washington, DC 20375-5320

NRL/MR/6350--98-8329

Optimimization of the Acoustic Performance of a Thick Plate with Embedded Actuators

C. T. DYKA

GEO-Centers, Inc.
Fort Washington, MD

G. C. KIRBY

Systems Analysis Branch
Spacecraft Engineering Department

December 31, 1998

REPORT DOCUMENTATION PAGE

Form Approved
OMB No. 0704-0188

1. AGENCY USE ONLY (*Leave Blank*)	2. REPORT DATE	3. REPORT TYPE AND DATES COVERED
	December 31, 1998	Final Report

4. TITLE AND SUBTITLE

Optimization of the Acoustic Performance of a Thick Plate with Embedded Actuators

5. FUNDING NUMBERS

6. AUTHOR(S)

C.T. Dyka* and G.C. Kirby†

7. PERFORMING ORGANIZATION NAME(S) AND ADDRESS(ES)

Naval Research Laboratory
Washington, DC 20375-5320

8. PERFORMING ORGANIZATION REPORT NUMBER

NRL/MR/6350--98-8329

9. SPONSORING/MONITORING AGENCY NAME(S) AND ADDRESS(ES)

DARPA
Arlington, VA 22209

10. SPONSORING/MONITORING AGENCY REPORT NUMBER

11. SUPPLEMENTARY NOTES

*GEO-Centers, Inc., P.O. Box 441340, Fort Washington, MD 20749
†Now in Code 8221

12a. DISTRIBUTION/AVAILABILITY STATEMENT

Approved for public release; distribution unlimited.

12b. DISTRIBUTION CODE

A

13. ABSTRACT (*Maximum 200 words*)

The acoustic response of a simple thick plate with embedded actuators is investigated in this work, and its performance optimized. (The actuators themselves are not modeled). The plate is subjected to an incident wave and the actuators (pistons) do not necessarily cover the entire plate. A standard minimization method as well as a genetic algorithm are used to minimize the acoustic intensity of the far field at both selected field points and the entire far field. A closed form solution is derived for the case of the actuators being driven at the same velocity amplitude, while a genetic algorithm is employed to find optimum solutions for the actuators being driven at different velocity amplitudes. The results indicate that the closed form solution, which can include actuators functioning below 100% capacity, produces excellent solutions when the plate is mostly covered with actuators. However, for plates that are only partially covered with actuators or if some of the actuators are not firing or well below 100%, the closed form approach can produce very poor results. The genetic algorithm generate viable solutions in all cases, but shows less spectacular improvements in the reduction of the far field intensities.

14. SUBJECT TERMS

Acoustics
Actuators
Genetic Algorithm
Optimization
Thick plates

15. NUMBER OF PAGES

28

16. PRICE CODE

17. SECURITY CLASSIFICATION OF REPORT	18. SECURITY CLASSIFICATION OF THIS PAGE	19. SECURITY CLASSIFICATION OF ABSTRACT	20. LIMITATION OF ABSTRACT
UNCLASSIFIED	UNCLASSIFIED	UNCLASSIFIED	UL

NSN 7540-01-280-5500

Standard Form 298 (Rev. 2-89)
Prescribed by ANSI Std 239-18
298-102

CONTENTS

OPTIMIZATION OF THE ACOUSTIC PERFORMANCE OF A THICK PLATE WITH EMBEDDED ACTUATORS

1. INTRODUCTION

The use of piezoelectric and other types of actuators embedded in structures to either control the structure, improve its performance or to reduce acoustic noise continues to grow. The modeling (see [1] for instance) and optimization of the global performance of these "smart structures" [2] is an important concern.

In this work, the focus will be on a simple plate with embedded piston type actuators subjected to an incident acoustic wave. The details of the actuators themselves are not modeled. They are assumed to be rectangular sources [3]. In addition, the actuators are assumed to cover a partial area of the plate with an impediance equal to that of the plate. This assumption could be relaxed. The present work relates to a smart panel designed for acoustic quieting. The smart panel was developed as part of the Composite Smart Materials (CSM) Program, which is an interdisciplinary effort involving several private corporations, academia and the Naval Research Laboratory [4].

Of primary concern in this work is the optimization/minimization of the acoustic intensity(or pressure) for the entire far field as well as in selected directions. In general, our approach is limited to steady state conditions because of the availability of simple closed form solutions for scattered and radiated pressures at specified frequencies. Transient solutions for this class of problems require detailed discretization of the fluid media which is computationally very costly, and lacks accuracy given the current state-of-the-art. In fact for an acoustic fluid, accurate general purpose transient boundary integral numerical solvers are presently not available although some progress has been made recently [5].

Optimization is itself a very broad topic. Rao [6] presents a good overview of optimization applied to enginnering problems. Unconstrained optimization techniques have been traditionally divided into two broad catagories – direct search methods, and descent or gradient methods [6,7]. Direct search methods require only the objective function values and not the partial derivatives in finding the minimum. The descent methods require derivatives of the objective function and are known as gradient methods.

Manuscript approved November 29, 1998.

Within the last few years several new methods have emerged. Among these are neural network techniques, simulated annealing and genetic algorithms. Neural network methods are based up the efficient computing power of the network of interconnected neuron processors. Simulated annealing [6,7] is analogous to the physical process of annealing of solids and has been successfully applied to a number of problems among them the traveling salesman problem [7]. It is well suited to problems of large scale, especially where a global minimum is hidden among many poorer solutions.

Genetic algorithms (GA) are search techniques based upon natural selection and genetics [8-10]. They can be quite robost and have been successfully applied to a number of difficult problems. We will be applying the GA to the problem considered here and will have more discussion of these methods in section 2.2.

2. FORMULATION

Consider the simple plate shown in Figure 1. The plate has dimensions $2L_x$ by $2L_y$, and several rectangular piston actuators are embedded. The dimensions of actuator m are a_m by b_m. Figure 1 indicates 4 of these macro-type actuators, which are comprised of groups of smaller pistons [4], but any reasonable number could be included. In addition, the actuators are not all necessarily at 100% capacity, nor do they necessarily provide coverage of the entire plate.

As indicated, plane wave of pressure P_{inc} impinges on the rectangular plate. P_{inc} is of the form:

$$P_{inc} = \bar{P}_{inc} e^{i(kr-\omega t)} \tag{1}$$

where $i = \sqrt{-1}$, t is the time, ω is the frequency in rad/s, $\bar{P}_{inc}$ is the pressure amplitude, r is the distance and k is the wave number defined by:

$$k = \omega / c \tag{2}$$

In equation (2), c is the speed of sound in the media.

The incident wave produces a scattered wave P_s at a field point which in spherical coordinates (r,θ,ϕ) is expressed as [3]:

$$P_s(r,\theta,\phi) = \frac{-i2k}{\pi r} e^{ikr} \bar{P}_i L_x L_y \cos\theta_i \cdot S(kL_x \cdot (\sin\theta_i \cos\phi_i + \sin\theta \sin\phi)) \tag{3}$$

$$\cdot S(kL_y \cdot (\sin\theta_i \cos\phi_i + \sin\theta \sin\phi))$$

where the function S has the form:

$$S() = \frac{\sin()}{()} \tag{4}$$

and θ_i and ϕ_i represent the orientation in spherical coordinates of the incident plane wave.

Referring to Figure 1 again, consider a typical actuator m with dimensions a_m by b_m and its centroid locationed at (x_{0m}, y_{0m}) within the plate. A local spherical coordinate system $(\bar{r}_m, \bar{\theta}_m, \bar{\phi}_m)$ is located at (x_{0m}, y_{0m}). From reference [3], the radiated pressure $P_{rad,m}$ produced by actuator m being driven at a complex velocity

$$v_m = \bar{v}_m e^{-i\omega t} \tag{5}$$

is:

$$P_{rad,m}(\bar{r}_m, \bar{\theta}_m, \bar{\phi}_m) = \bar{v}_m \cdot \bar{P}_{rad,m}(\bar{r}_m, \bar{\theta}_m, \bar{\phi}_m) \tag{6}$$

In equations (5) and (6), $\bar{v}_m$ is the velocity amplitude and $\bar{P}_{rad,m}$ is defined as:

$$\bar{P}_{rad,m}(\bar{r}_m, \bar{\theta}_m, \bar{\phi}_m) = -2i\omega\rho \bar{v}_m \cdot (a_m/2) \cdot (b_m/2) \cdot S(.5ka_m \sin\bar{\theta}_m \cos\bar{\phi}_m) \tag{7}$$

$$S(.5kb_m \sin\bar{\theta}_m \sin\bar{\phi}_m) \cdot e^{ik\bar{r}_m} / (4\pi\bar{r}_m)$$

In the calculations, a field point is expressed in the global spherical coordinates (r, θ, ϕ) and then transformed to the m actuator local spherical coordinates to determine $\bar{P}_{rad,m}$.

2.1 A Standard Mimimization Approach

With the scattered solution P_s from equation (3) and the radiated solution $P_{rad,m}$ from actuator m given by equations (6-7), the total pressure at a typical field point (r, θ, ϕ) can be expressed by:

$$P_{tot}(r, \theta, \phi) = P_s(r, \theta, \phi) + \sum_{m=1}^{M} P_{rad,m}(r, \theta, \phi) \tag{8}$$

In this equation, the M actuators may or may not cover the entire plate. Assuming for the moment that all the actuators are being driven at the same velocity amplitude $\bar{v}$, equation (8) can be rewritten as:

$$P_{tot}(r,\theta,\phi) = P_s(r,\theta,\phi) + \bar{v}\sum_{m=1}^{M} f_m \bar{P}_{rad,m}(r,\theta,\phi) \tag{9}$$

The factor f_m varies between 0 and 1 and allows for the case of actuator m operating at less than 100% capacity.

Assuming there are N_f field points of interest in the far field, equation (9) can be written in vector form as:

$$\underline{P}_{tot} = \underline{P}_s + \bar{v}\cdot\underline{\underline{P}}_{rad} \tag{10}$$

where

$$\underline{\underline{P}}_{rad} = \sum_{m=1}^{M} f_m \underline{\underline{F}}_w \underline{P}_{rad,m} \tag{11}$$

In equation (11), $\underline{\underline{F}}_w$ is a matrix that allows the field point locations to be weighted if desired.

We next define a performance scalar J_P that is proportional to the summation of the acoustic intensities of the far field [3] as:

$$J_P = \hat{\underline{P}}_{tot}^{T} \bullet \underline{P}_{tot} \tag{12}$$

where $\hat{\underline{P}}_{tot}^{T}$ implies the transpose of the complex conjugate of the vector $\underline{P}_{tot}$. Introducing equations (10-11) into (12) produces:

$$J_P = \hat{\underline{P}}_s^{T} \bullet \underline{P}_s + \hat{\underline{\underline{P}}}_{rad}^{T} \bullet \underline{P}_s + \bar{v}\cdot\underline{P}_s^{T} \bullet \underline{\underline{P}}_{rad} + \bar{v}^2 \hat{\underline{\underline{P}}}_{rad}^{T} \bullet \underline{\underline{P}}_{rad} \tag{13}$$

From [11], the minimum value of $\bar{v}$ is determined by:

$$\bar{v}_{min} = -(\hat{\underline{\underline{P}}}_{rad}^{T} \bullet \underline{P}_s)/(\hat{\underline{\underline{P}}}_{rad}^{T} \bullet \underline{\underline{P}}_{rad}) \tag{14}$$

The real part of equation (14) represents the velocity amplitude for all the actuators (some may not be at 100%) to minimize the summation of the acoustic intensities at the specified number of far field parts. In this work, we will refer to $\bar{v}_{min}$ produced by equation (14) as the closed form minimum (CFM) velocity.

It has been our experience that if there is a significant imaginary component of $\bar{v}_{min}$, the solution is quite poor. This indicates that an optimized solution with all the actuators having the same velocity amplitudes may not possible, or at the very least, require the introduction of some phase differences in the actuators.

The equations in this section were programed and solved using the commercially available MATLAB program [12-13]. In addition to selected field points, our resulting code can also include the acoustic intensity of the entire far field at a specified radius r. The program sets up in MATLAB a grid of N_{f1} field points at r which covers the limits of θ and ϕ. The J_P calculation can be then put in the form:

$$J_p = A\ J_{p1} / N_f + B\ J_{p2} / N_{f1} \tag{15}$$

where A and B vary from 0 to 1 and sum to 1; and J_{p1} and J_{p2} represent the summations that are proportional to the intensities of all specified field points N_f and from the grid of N_{f1} field points covering the entire far field, respectively.

Returning to equations (9) and (11), one can allow all the individual actuators to be driven at different amplitudes $\bar{v}_m$. Equation (9) then becomes:

$$P_{tot} = P_s + \sum_{m=1}^{M} f_m \bar{v}_m \bar{P}_{rad,m} \tag{16}$$

For N_f field points, equation (16) can be written in a form similar to (10) or

$$\underline{P}_{tot} = \underline{P}_s + \underline{\bar{v}} \cdot \underline{\underline{\bar{P}}}_{rad,M} \tag{17}$$

where $\underline{\bar{v}}$ is now the vector of the actuator velocity amplitudes, and $\underline{\underline{\bar{P}}}_{rad,M}$ is a matrix of the radiated pressures with dimensions N_f by M. With (17), an equation similar to (12) can be generated for the performance scalar J_p. Application of standard gradient type techniques [6,7,14] can then be introduced to solve for the optimized minimum of the actuator velocities. Our experience with standard gradient techniques, however, proved very disappointing. The solutions became stuck in local minimums unable to explore possibly better solutions over a much larger solution space.

2.2 A Genetic Algorithm

Genetic algorithms (GA's) represent a type of stochastic search approach that attempts to mimic nature. GA's are well suited for the solution of many optimum design problems that are characterized by mixed continuous/discrete variables, and large discontinuous and nonconvex solution spaces [6]. Expensive gradient calculations are not needed for GA's, but the evaluation of individual performances must be inexpensive and fast for a genetic algorithm to be effective. For the class of problem we are investigating in this work, these above conditions are satisfied.

GA's are based upon the principles of genetics and natural selection. Basic ingredients in these types of numerical algorithms include reproduction, crossover and mutation capabilities.

For the problem considered in this work, the design variables will be the velocity amplitudes $\bar{v}_m$ of the indivdual actuators. The velocity amplitudes are transformed into strings of binary numbers, 0 or 1. We assume here that each string is 6 bits long allowing $2^6 = 64$ possible discrete values for each actuator. In our MATLAB generated program, both lower and upper velocity amplitudes, vel1 and vel2, are specified for all the actuators. The range of velocities between and including vel1 and vel2 is divided into 64 slots and encoded as binary strings. Figure 2 indicates an example having 4 actuators. A 6 bit binary string for each actuator velocity is shown along with its translation into the appropriate velocity slot. This 24 bit string of four, 6 bit strings represents an individual in the total population.

Reproduction is a process in which individuals are selected to be parents base upon their fitness measure (such as J_p in equation (13)) relative to the rest of the population. Each individual 24 bit string j is assigned a probability of being selected for reproduction via

$$\mathrm{Prob}_j = J_{p,j} / \sum_{jj=1}^{N} J_{p,jj} \tag{18}$$

where $J_{p,j}$ is the performance or fitness of each individual and N is the size of the population. Highly fit individuals have a greater chance for reproduction, while less fit ones tend toward extinction.

Parent 1, x_1, and parent 2, x_2, will produce two offspring y_1 and y_2. A crossover site is then selected at random along the string lengths, and the binary digits are swapped between the two strings following the crossover site. The new strings y_1 and y_2 are then placed in the new population and the process continued until N individuals are generated for the next generation.

A mutation operator is also included for the new string in which there is an occasional random alteration of a binary digit in the string from a 0 to a 1, or 1 to 0. This is controlled by a mutation probability that is usually set low (a few percent). Mutation is a needed ingredient because even though reproduction and crossover effectively search and recombine strings, occasionally some important genetic information can be lost, or the solution can be trapped at local minimums. The mutation operator helps to prevent this, and also introduces new possibilities, some of which can be improvements, into the population.

For the GA, a performance scalar J_P defined by equation (12) rather than (15) was employed. N_f selected field points were again specified for the far field, but a J_{P2} term was not included due to the excessive computational cost that would be required – every member of the population in every generation would require the calculation of the J_{p2} term.

Another point to be mentioned concerns the scaling of the performance (fitness) $J_{p,j}$ for each individual in the population. Outstanding individuals can tend to dominate then saturate a population early and prevent the evolution of more fit individuals. If this occurs, the solutions become stuck at local minimums and are unable to more fully explore a wider range of the solution space. One simple way to help alleviate this situation is to modify $J_{p,j}$ by raising it to a power x_n, which typically is in the range $0+ \leq x_n \leq 1.0$. The quantity x_n varies depending upon the generation number n. For the early generations, x_n is set to some specified lower limit and scaled to the upper limit for the last generation. Later in an optimization run x_n approaches the upper limit, and this allows the more fit individuals to then saturate the population.

Finally, we note that because genetic algorithms are based upon probability many times it is necessary to make several computer runs to obtain best results. In the following section, this is implicit in the discussion of the results.

3. RESULTS AND DISCUSSION

Consider the simple plate with 4 symmetrically placed actuators as shown in Figure 1. (The numbering of the actuators begans at one for the first quadrant then proceeds in a counterclockwise or ϕ direction). An incident wave P_{inc} in the form of equation (1) impinges on the square plate. The following values were assumed: $\bar{P}_{inc} = 10$ Pa, $\theta_{inc} = \pi/6$ rad, $\phi_{inc} = 0$ rad, and ω = 500 rad/s for the incident wave; $L_x = L_y$ = 1 m, a=b=.3 m for the plate and actuators; and c = 1500 m/s, and ρ = 1000 kg/m^3 for the fluid media. Figures 3 and 4 are intensity J_P (given by equation (12)) plots for the entire far field at a distance of r=500 m for the closed form minimum (CFM) solution from equation (14); and the GA. For both solutions, the minimization calculations were executed with r=500 m and with 4 field points $\theta = \pi/6$ and $\phi = (0, \pi/2, \pi/6, \pi/2)$. Figure 5 is a baseline plot of the far field with all of the actuators off.

The CFM solution, which is shown in Figure 3, calculated a minimum actuator velocity of 5.17×10^{-5} m/s and yielded decibel (dB) reductions of the intensities of the entire far field and 4 field points of –7.4 dB, and –3.34, -36.2, -10.3, and –36.2 dB, respectively. The decibel calculations are determined from the formula $10*\log(I/I_{ref})$, where I and I_{ref} represent the acoustic intensities with the actuators on and off [15] . Many other combinations of various field point locations were tried as well as including the entire far field via equation (15), and selecting different values of A and B. The results in Figure 4 are representative of the best overall minimization of the far field by the CFM. In general, the selection of far field points in direction other than $\theta = \pi/6$ improved those particular directions only so much with minimum impact on the reduction of the entire far field acoustic intensity.

Figure 4 indicates about the best results obtained via the genetic algorithm for r=500 m with 4 field points $\theta = \pi/6$ and $\phi = (0, \pi/2, \pi/6, \pi/2)$. The population size for the

GA was 200, the number of generations were 70, and a fairly high mutation factor of 0.10 was used. The predicted actuator velocites obtained were: $.794 \times 10^{-5}$, 9.05×10^{-5}, 8.41×10^{-5}, and 1.27×10^{-5} m/s. The dB reductions were –3.79 for the entire far field, and –4.6, -7.1, -9.3 and –7.2 dB for the 4 field points. In obtaining these results, the GA was limited to actuator velocities between 0 and 10.0×10^{-5} m/s. Limiting to the GA to a narrower range closer to the CFM results of approximating 5.0×10^{-5} m/s produced GA solutions closer and closer to this optimum number.

Overall, based on these and numerous other results for both the CFM and the GA, we conclude that firing all the 4 actuators at approximately 5.0×10^{-5} m/s produced the best overall solution for this symmetric problem.

We next consider the same plate and incident loading with again 4 actuators, but this time the actuators were running at 100, 75, 10 and 50% efficiencies, respectively. The far field intensities J_P were optimized/minimized for 8 field points or: $(\theta, \phi) = (\pi/2,0)$, $(\pi/2,\pi/2)$, $(\pi/2,\pi)$, $(\pi/2, 1.5\pi)$, $(\pi/6,0)$, $(\pi/6,\pi/2)$, $(\pi/6,\pi/2)$ and $(\pi/6,1.5\pi)$. Figures 6 and 7 indicate the CFM and GA J_P (equation (12)) results. Although quite dissimilar in shape, the CFM and GA results are very close in the overall reduction of the intensity of the entire far field . The dB reductions were –4.48 and –4.45, respectively. For these GA results, the population size was 400 and there were 100 generations, along with a mutation factor of 5%. The predicted actuator velocities for the GA were 7.62×10^{-5},4.38×10^{-5}, 9.90×10^{-5}, and 11.81×10^{-5} m/s. The CFM predicted a uniform velocity of 9.66×10^{-5} m/s with a significant imaginary component of $.533 \times 10^{-5}$ m/s.

Actuators 2 and 3 (the second and third quadrants) were then completely turned off, producing an even more unsymmetric arrangement. The CFM results contained an imaginary component in the velocity of actuators 1 and 4 that was approximately 25% of the real part. This represented a very poor solution that actually increased the intensity significantly in the entire far field.

Figure 8 shows the results from the GA with actuators 2 and 3 turned off. The GA produced a dB reduction of the entire far field of –3.4 dB with actuator velocities of 7.16×10^{-5} and 7.00×10^{-5} m/s, respectively.

Using only the genetic algorithm, we next consider the situation of 16 symmetrically placed actuators, of the same dimensions as before with a=b= .3 m, embedded in the

plate. To keep the actuator velocities similar in magnitude to the previous 4 actuator models, the magnitude of the incident wave P_{inc} was increased from 10 to 40 Pa, while its direction remained the same $\theta_{inc} = \pi/6$ rad and $\phi_{inc} = 0$ rad, and ω = 500 rad/s. The far field intensities were optimized at 4 field points $\theta = \pi/6$ and $\phi = (0, \pi/2, \pi/6, \pi/2)$. The population size was 200 and 70 generations were run. The GA produced actuator velocities of (1.43,3.49,3.97, 5.87, 2.38, 8.10, 8.25, 8.73, 8.89, 7.94, 9.84, 7.62, 6.51, 3.97, 1.43, 10.0)x10^{-5} m/s. Figure 9 is a plot of the entire far field at r=500 m, and Figure 10 is a plot with all the actuators off. The decibel reductions were –6.42 dB for the entire far field, and +.178 (increase), -13.76, -14.8, and –13.7 dB for the selected field points. Comparing these results to those of the 4 actuator model of Figure 4, we see that the shape of the far field has changed considerably and the dB reductions are greater than previous at every point other than the first field point $(\theta, \phi) = (\pi/6, 0)$.

Finally, we investigate the case of 16 actuators on the plate, but with numbers 9-16 turned off completely (the entire second and third quadrants). In an attempt to cover more of the far field, 24 field points were selected with θ and ϕ varying from $\theta = (\pi/2, \pi/4, \pi/6)$ and $\phi = (0, \pi/4, \pi/2, .75\pi, \pi, 1.25\pi, 1.5\pi, 1.75\pi)$. Following several runs, the best optimized velocities produced by the GA for the actuators 1 – 8 were (1.67, .71, 1.67, 6.67, 5.95, 13.81, 10.95, 13.57) x10^{-5} m/s. Figure 11 indicates the entire far field acoustic intensity at r=500 m. The decibel reduction for the entire far field was computed as –4.7 dB, which was actually quite good considering half the actuators are turned off. Note, however, that as in Figure 9, along $\phi = 0$ the intensities J_P have increased slightly.

4. CONCLUSIONS

In this work, we have considered a simple thick plate with embedded piston type actuators that is impinged upon by an acoustic incident wave. The actuators do not necessarily cover the entire plate nor operate at 100%. The question addressed concerns the optimization /minimization of the acoustic intensity of the far field – either in specific directions or the entire far field.

A standard minimization approach was first employed to address this problem. A closed form minimum (CFM) was obtained for the situation in which the actuators are all being driven at the same velocity amplitude. The reductions in the far field were excellent for the situation where most of the plate is covered and the actuators were all running at near 100% capacity. For even some moderate non-symmetry in the problem, such as indicated in the discussion for Figure 6, the CFM produced reasonable results. However, the CFM results declined substantially producing erroneous solutions when significant non-symmetry was introduced into the problems. In these cases, equation (14) generated results for $\bar{v}_{min}$ with substantial imaginary components. This indicated that an optimized solution with all the actuator velocity amplitudes the same may not be feasible, or at the very least, requires the use of phase differences in the individual actuator responses.

The use of standard gradient type of techniques for the case of the actuators be driven at different velocity amplitudes proved to be ineffective. Solutions became trapped at local minimums unable to explore larger solution spaces.

The genetic algorithm was successfully applied to all the cases considered in this work. The GA produced feasible solutions in which all the actuators were driven at different velocity amplitudes (although groups of actuators could have been tied together if desired). For a symmetric situation the GA produced smaller dB reductions than the CFM. However, unlike the CFM, the GA generated viable solutions for the reduction of the far field acoustic intensities in all cases tried, including the most unsymmetric situations.

Results for both the CFM and GA approaches revealed that only limited improvement in the far field intensity reduction was possible for either specific directions or the entire far field. In addition to the results reported in this work in which θ_{inc} and ϕ_{inc} were fixed at $\pi/6$ and 0 radians, respectively, numerous other values and combinations of actuators were examined. Those results tended to agree with this statement. However, by no means did we conduct an exhaustive numerical study.

In the future, we plan on seeking to include delays in the actuator responses in both the CFM and GA form of the equations. This should improve the results especially for highly non-symmetric situations, and allow further reductions in specific directions by steering the response into other directions [15].

5. ACKNOWLEDGMENTS

The authors would especially like to thank Dr. Peter Matic, Head of Section 6382 at NRL, for his encouragement and support of this work. The support of Dr. R. Crowe and the Defense Advanced Research Projects Agency (DARPA) is gratefully acknowledged. The second author was also partially supported by the Office of Naval Research (ONR).

6. REFERENCES

1. V .G. DeGiorgi 1997 *Adaptive Structures and Material Systems*, ASME, AD-Vol 54, Host-active component interactions and performance predictions.
2. M. V Gandhi and B. S. Thompson 1992 *Smart Materials and Structures*. New York: Chapman and Hall.
3. M. C. Junger and D. Feit 1986 *Sound, Structures and Their Interaction*. New York: Chapman and Hall.
4. *CSM Quarterly Report* , Lockheed Martin MS-ATC to the Office of Naval Research, January 1997.
5. C. T. Dyka, R. P. Ingel and G. C. Kirby 1997 *International Journal for Numerical Methods in Engineering* **40**, 3767-3783. Stabilizing the retarded potential method for transient fluid-structure interaction problems.
6. S. S. Rao 1996 *Engineering Optimization, Theory and Practice*. New York: Wiley, third edition.
7. W. H. Press, S. A. Teukolsky, W. T. Vettering and B. P. Flannery 1992 *Numerical Recipes in Fortran, The Art of Scientific Computing*. New York: Cambridge University Press, second edition.
8. D. E. GoldBerg 1989 *Genetic Algorithms in Search, Optimization, Machine Learning*. Reading: Addison-Wesley.
9. A. K. Dhindra and B. H. Lee 1994 *International Journal for Numerical Methods in Engineering* **37**, 4059-4080. A genetic algorithm approach to single and multiobjective structural optimization with discrete-continuous variables.

10. M. Galante 1996 *International journal for Nummerical Methods in Engineering* **39**, 361-382. Genetic algorithms as an approach to optimize real-world trusses.

11. P. A. Nelson and S. J. Elliot 1992 *Active Control of Sound.* New York: Academic Press pg. 240.

12. *MATLAB, High Performance Numeric Computation and Visualization Software, User's Guide.* Natick: The MathWorks, Inc. 1992.

13. R. Pratap 1996 *Getting Started with MATLAB, A Quick Introduction.* New York: Harcourt.

14. A. Grace 1994 *Optimization TOOLBOX for Use with MATLAB User's Guide.* Natick: The Math Works, Inc.

15. L. E. Kinsler, A. R. Frey, A. B. Coppens and J. V. Sanders 1982 *Fundamentals of Acoustics.* New York: Wiley, third edition.

7. LIST OF FIGURES

8) Figure 8. GA results for 4 actuators with numbers 2 and 3 (second and third quadrants) completely off. Decibel reduction = -3.4 for the entire far field.

9) Figure 9. GA results for 16 symmetrically placed actuators. Decibel reduction = -6.42 for the entire far field.

10) Figure 10. Baseline, all 16 actuators are off.

11) Figure 11. GA results for 16 actuators with numbers 9-16 (second and third quadrants) completely off. Decibel reduction = -4.7 for the entire far field.

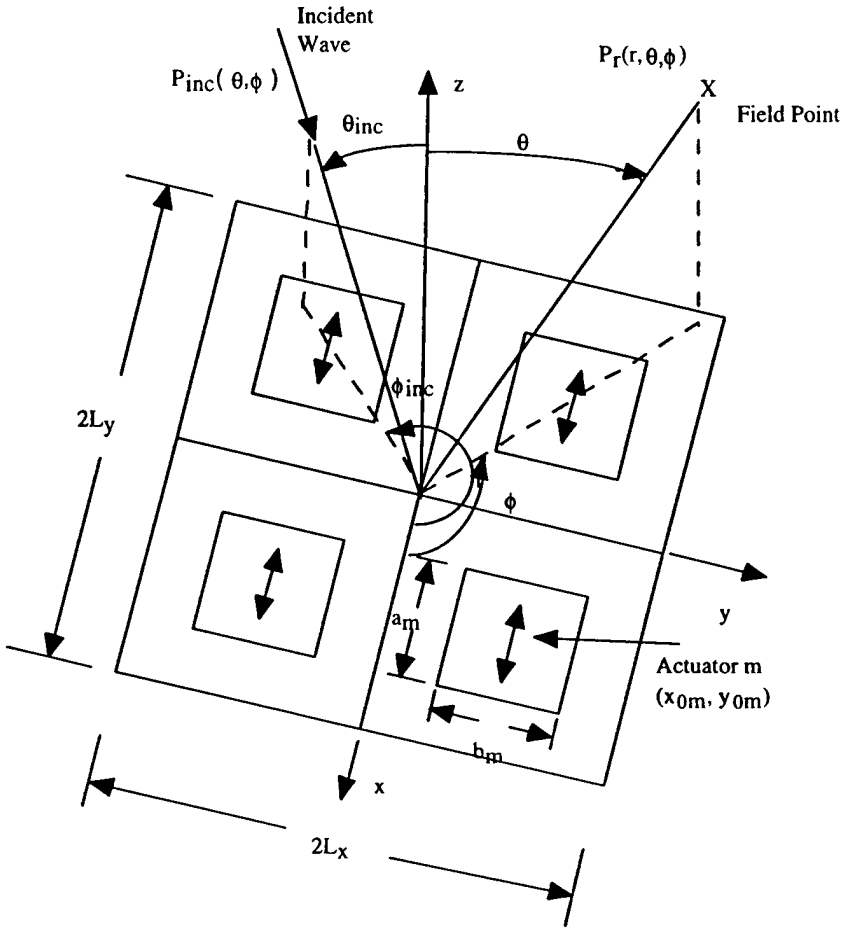

Figure 1. Simple plate with embedded actuators.

•Actuator with variable velocities (acoustic solution, same frequency)

• Each actuator up to $2^6 = 64$ possible velocities - 6 bits

Actuator Number (assume 4 actuators in problem)

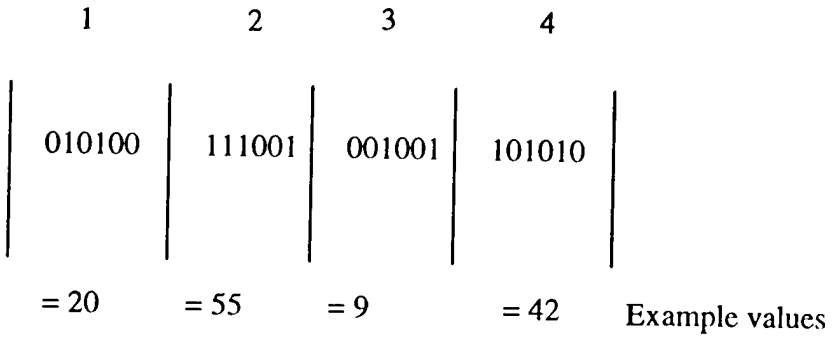

Figure 2. Example of the conversion of individual actuator velocities to binary strings for the GA.

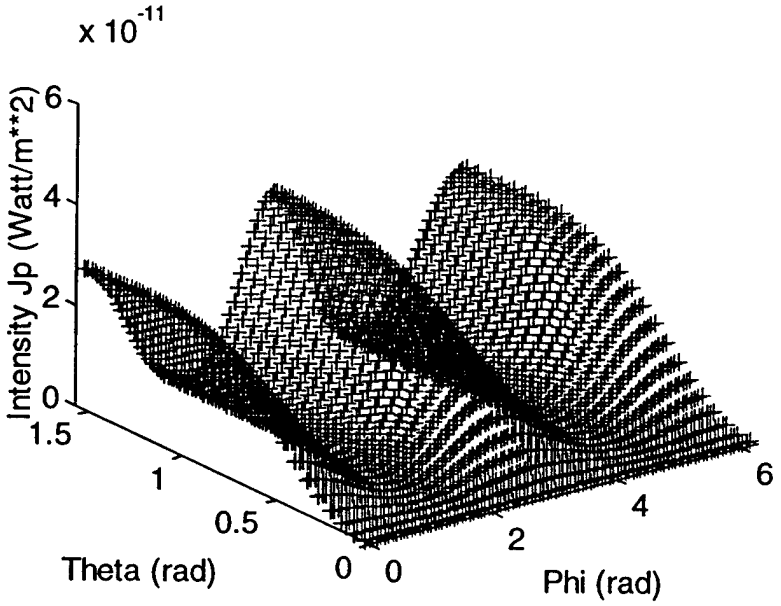

Figure 3. CFM intensity results for 4 symmetrically placed actuators. Decibel reductions: total intensity of far field = -7.4; selected field points = -4.6, -36.2, -10.3, and –36.2

.

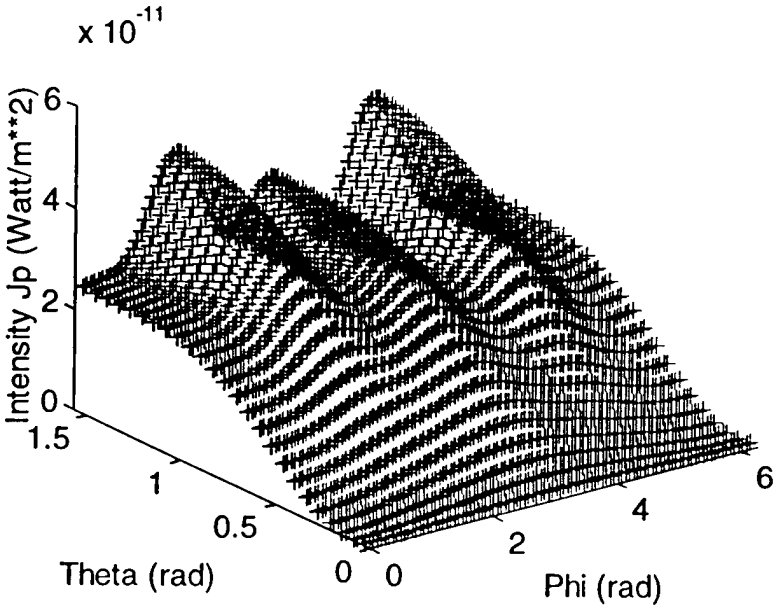

Figure 4. GA intensity results for 4 symmetrically placed actuators. Decibel reductions: total intensity of far field = -3.8; selected field points = -4.6, -7.1, -9.3, and –7.2 .

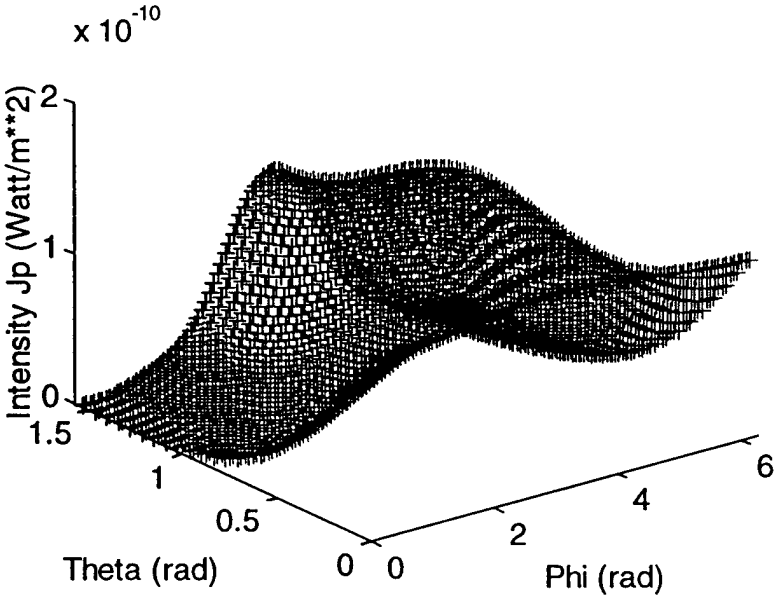

Figure 5. Baseline, all 4 actuators are off.

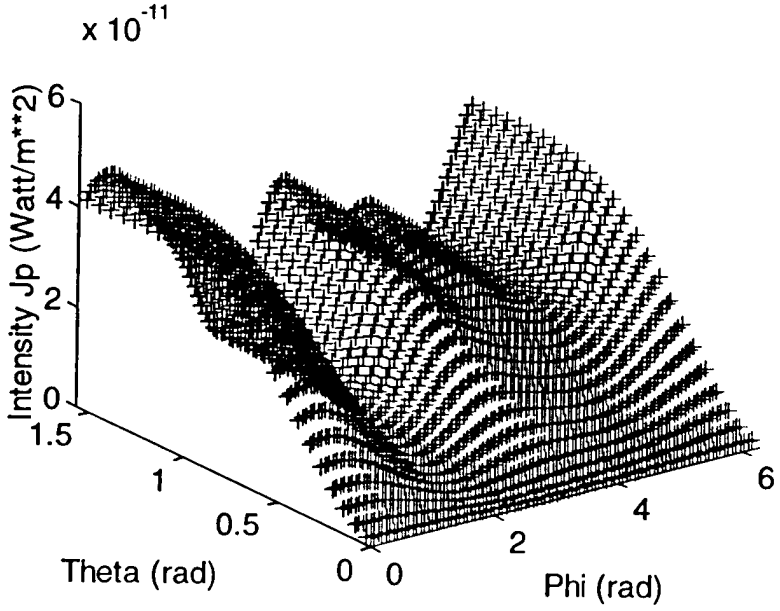

Figure 6. CFM intensity results for 4 actuators running at 100, 75, 10 and 50% efficiencies. Decibel reductions: total intensity of the entire far field = -3.8; selected field points = -4.6, -7.1, -9.3, and –7.2 .

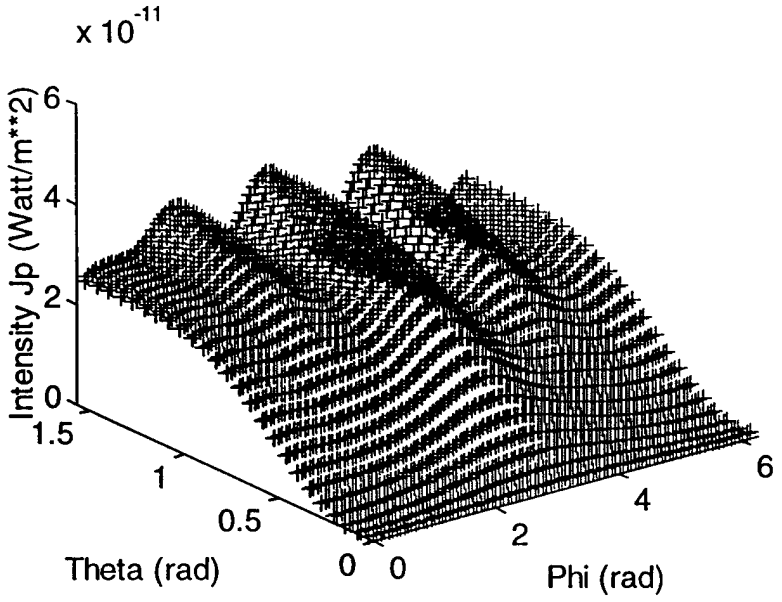

Figure 7. GA results for 4 actuators running at 100, 75, 10 and 50% efficiency. Decibel reduction = -4.45 for the total intensity of the entire far field.

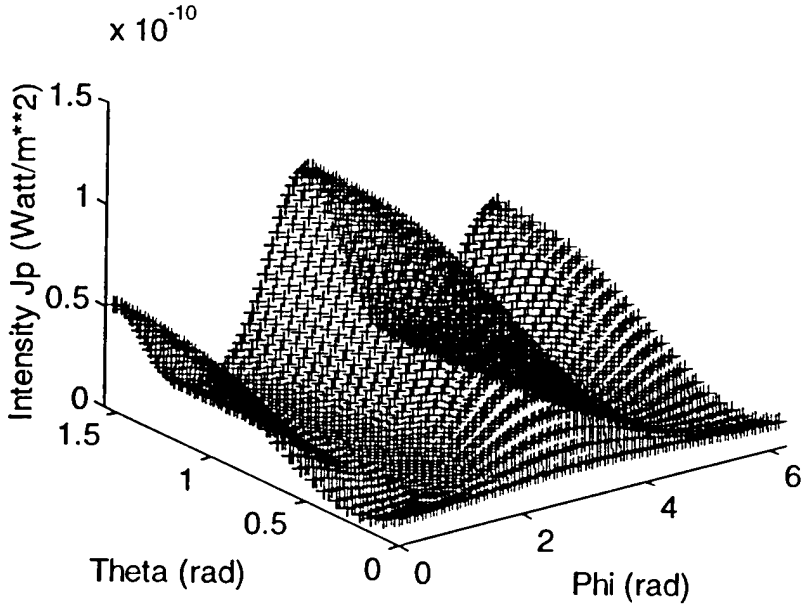

Figure 8. GA results for 4 actuators with numbers 2 and 3 (second and third quadrants) completely off. DB reduction = -3.4 for the entire far field.

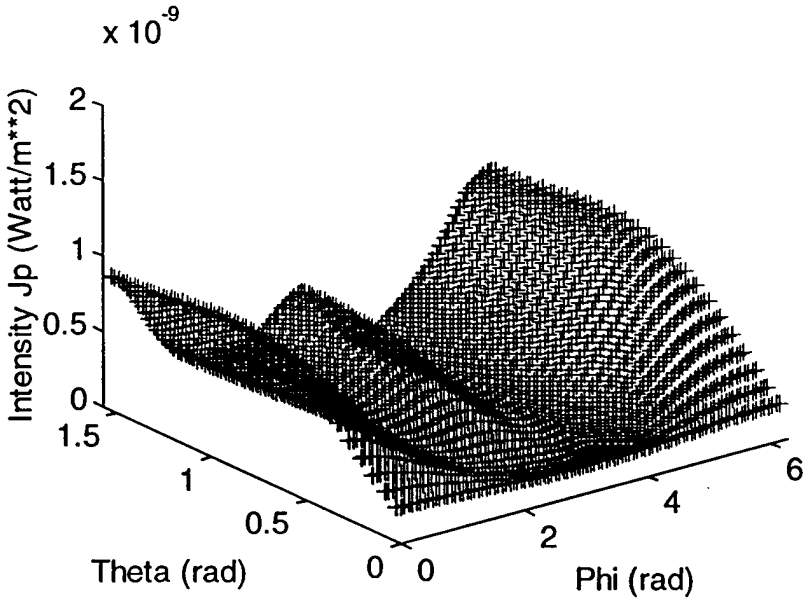

Figure 9. GA results for 16 symmetrically placed actuators. Decibel reduction = -6.42 for the entire far field.

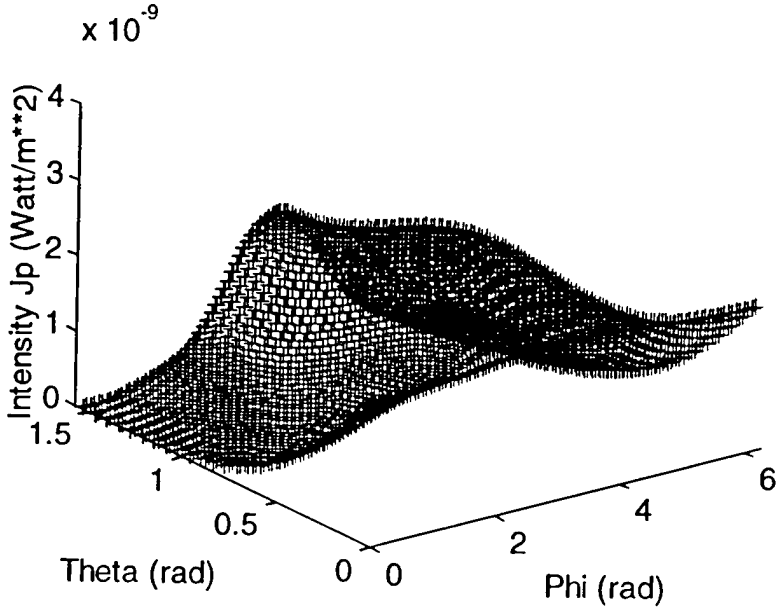

Figure 10. Baseline, all 16 actuators are off.

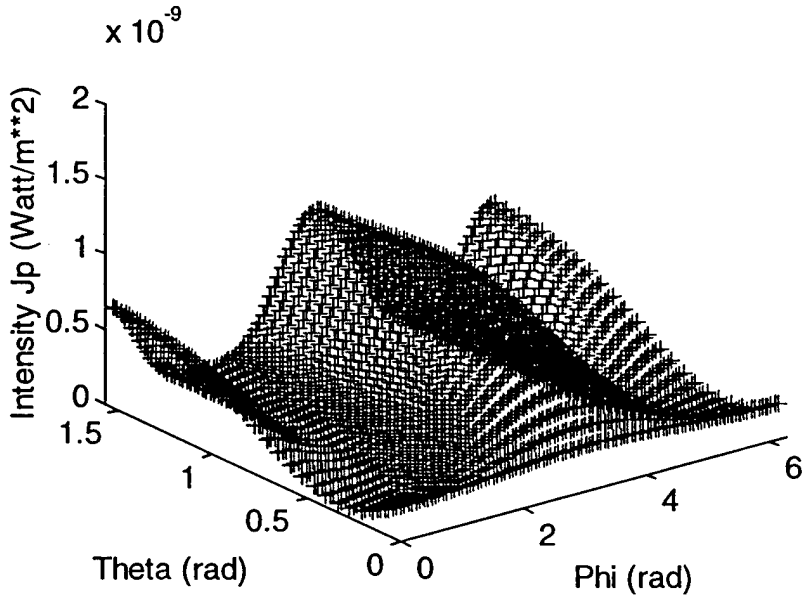

Figure 11. GA results for 16 actuators with numbers 9-16 (second and third quadrants) completely off. Decibel reduction = -4.7 for the entire far field.